Europe PMC Funders Group
Author Manuscript
Mucosal Immunol. Author manuscript; available in PMC 2013 September 01.

Published in final edited form as:
Mucosal Immunol. 2013 September ; 6(5): 1027–1037. doi:10.1038/mi.2012.141.

The functional maturation of M cells is dramatically reduced in the Peyer's patches of aged mice

Atsushi Kobayashi[1,2,*], **David S. Donaldson**[1,*], **Clett Erridge**[3], **Takashi Kanaya**[4], **Ifor R. Williams**[5], **Hiroshi Ohno**[4], **Arvind Mahajan**[1], and **Neil A. Mabbott**[1,#]

[1]The Roslin Institute & Royal (Dick) School of Veterinary Sciences, University of Edinburgh, United Kingdom

[2]Tohoku University Graduate School of Medicine, 2-1 Seiryo-machi, Aoba-ku, Sendai, Japan

[3]Department of Cardiovascular Sciences, University of Leicester, Leicester LE3 9QP, United Kingdom

[4]Research Center for Allergy and Immunology (RCAI), RIKEN, 1-7-22 Suehiro, Tsurumi, Yokohama 230-0045, Japan

[5]Department of Pathology, Emory University School of Medicine, Whitehead Bldg. 105D, 615 Michael St., Atlanta, GA 30322, USA

SUMMARY

The transcytosis of antigens across the follicle-associated epithelium (FAE) of Peyer's patches by microfold cells (M cells) is important for the induction of efficient immune responses to mucosal antigens. The mucosal immune response is compromised by ageing, but effects on M cells were unknown. We show that M-cell density in the FAE of aged mice was dramatically reduced. As a consequence, aged Peyer's patches were significantly deficient in their ability to transcytose particulate lumenal antigen across the FAE. Ageing specifically impaired the expression of Spi-B and the down-stream functional maturation of M cells. Ageing also dramatically impaired CCL20 expression by the FAE. As a consequence, fewer B cells were attracted towards the FAE, potentially reducing their ability to promote M-cell maturation. Our study demonstrates that ageing dramatically impedes the functional maturation of M cells, revealing an important ageing-related defect in the mucosal immune system's ability to sample lumenal antigens.

INTRODUCTION

The gastrointestinal tract is continuously exposed to large amounts of microorganisms. As well as mounting an effective immune response against food-borne pathogens, the mucosal immune system must also recognise the harmless antigens associated with food and commensal microorganisms and generate immunological tolerance against them. The lumenal surface of the intestine limits the access of pathogenic microorganisms to the underlying host tissues, and is protected by a single layer of epithelial cells bound by tight-junctions. In order to mount an immune response, gut luminal antigens must first be transported across the intestinal epithelium. Located within the specialized follicle-associated epithelia (FAE) overlying the GALT such as Peyer's patches and isolated

[#]Correspondence: The Roslin Institute & Royal (Dick) School of Veterinary Sciences, University of Edinburgh, Easter Bush, Midlothian EH25 9RG, United Kingdom Tel: +44 (0)131 651 9100 Fax: +44 (0)131 651 9105 neil.mabbott@roslin.ed.ac.uk.
[*]Authors contributed equally to this study.

The authors declare no competing financial conflict of interest.

Europe PMC Funders Author Manuscripts
Europe PMC Funders Author Manuscripts

Europe PMC Funders Author Manuscripts

Europe PMC Funders Author Manuscripts

lymphoid follicles are microfold cells (M cells). This unique subset of epithelial cells is specialized for the transcytosis of lumenal macromolecules, particulate antigens and pathogenic or commensal microorganisms[1-3]. Following their uptake and transcytosis by M cells, antigens exit into the intraepithelial pocket beneath the basolateral membrane where they are subsequently processed by macrophages and classical dendritic cells (DC). In the absence of M cells, antigen-specific T cell responses in the Peyer's patches of mice orally-infected with *Salmonella* Typhimurium are significantly impaired[4].

The mucosal immune response in the intestine is significantly compromised by ageing[5-8]. The age-related decline in immune competence is associated with diminished antigen-specific IgA antibody titres in the intestinal lumen[6, 9] and a decreased ability to generate tolerance to harmless antigens[7]. The age-related increases in the incidence and severity of gastrointestinal infections, cancer, inflammatory diseases, coupled with decreases in the efficacy of vaccinations, illustrate the importance of studies aimed at understanding the factors involved in this immunosenescence. Many studies have addressed the age-related changes to systemic immune responses, particularly the ageing effects on T cell responses, but little is known of the mechanisms underlying the decline in intestinal immunity.

The transcytosis of antigens by M cells is an important initial step in the induction of efficient immune responses to certain antigens such as microorganisms. Furthermore, the targeted delivery of vaccine antigens to M cells has been shown to be an effective means of inducing antigen-specific immune responses[10, 11]. However, despite the important role of M cells in mucosal immunity, nothing was known about the effects of ageing on their development and function. The identification of the cellular and molecular factors affected in the senescent mucosal immune system is crucial for the development of mucosal vaccines and effective strategies to improve intestinal immunity in the aged. Therefore, in the current study a mouse model was used to determine the effects of ageing on M-cell status. Our data show for the first time that there is a dramatic decline in the functional maturation of M cells in the Peyer's patches of aged mice.

RESULTS

M-cell density is significantly reduced in the FAE of aged mice

First we used whole-mount immunohistochemistry (IHC) to compare the number of M cells in the FAE of Peyer's patches from young adult (6-8 weeks old) and aged C57BL/6J mice (≥ 18 months old). Glycoprotein 2 (GP2) is a specific surface marker for mature M cells[12, 13]. As anticipated, large numbers of $GP2^+$ M cells with characteristic basolateral pockets were detected in the FAE of Peyer's patches of young mice. However, the number of $GP2^+$ M cells in the FAE of aged mice was dramatically and significantly reduced (Figures 1a and b; $P < 0.0001$, Mann-Whitney U test). The number of M cells in the FAE of aged mice was < 25% that observed in young mice. Real-time quantitative PCR analysis showed there was also a significant reduction in *Gp2* mRNA expression in Peyer's patches from aged mice (Figure 1c; $P < 0.022$, Student's t-test).

Although the number of Peyer's patches was not affected by host age[14], morphometric analysis suggested that the size of the FAE in those from aged mice was typically 30% smaller (Figure 1d; $P < 0.0039$, Student's t-test). However, the reduced number of M cells in aged Peyer's patches was not simply due to a reduction in the overall size of the FAE, since the density of M cells in aged mice was also significantly reduced (Figure 1e; $P < 0.001$, Mann-Whitney U test). In contrast to the effects of ageing on M cells, the density of goblet cells recognised by their morphology, lack of GP2-expression and binding of the lectin *Ulex europaeus* agglutinin-1 (UEA-1; $GP2^-UEA\text{-}1^+$ cells) in the FAE of aged mice was similar to

Europe PMC Funders Author Manuscripts

Europe PMC Funders Author Manuscripts

that observed in the FAE of young mice (Figure 1f; $P = 0.704$, Student's t-test). These data demonstrate that M cell density is dramatically reduced in the FAE of aged mice.

The uptake of particulate antigen into the Peyer's patches of aged mice is significantly impaired

We next determined whether the reduced density of $GP2^+$ M cells in the FAE of aged mice correlated with effects on the uptake of particulate antigen from the gut lumen. The assessment of the uptake of fluorescent latex beads injected into ligated loops of the small intestine is a useful quantitative method to compare the functional ability of M cells *in vivo* to take up particulate antigen from the gut lumen and transcytose them to underlying mononuclear phagocytes in their intraepithelial pockets[2, 15]. Peyer's patches in groups of young and aged mice were surgically ligated and injected with fluorescent 200 nm latex beads. The Peyer's patches were then removed 1 h after injection and the number of beads taken up into each tissue quantified microscopically. In Peyer's patches from young mice many fluorescent beads had been transcytosed across the FAE (Figure 2). However, in tissues from aged mice substantially fewer, if any, beads had passed through the FAE (Figure 2; $P < 0.0061$, Student's t-test).

RANKL and RANK expression are not adversely affected in the Peyer's patches of aged mice

The production of receptor activator of NF-κB ligand (RANKL) by the subepithelial stromal cells beneath the FAE is a critical factor that stimulates the differentiation of receptor activator of NF-κB (RANK)-expressing enterocytes into M cells[2]. Since M cells are depleted *in vivo* by RANKL neutralization, and are absent in RANKL-deficient mice, we determined whether the reduced M-cell density in aged mice was due to impaired RANKL-stimulation. No difference was observed in the expression or distribution of RANKL in Peyer's patches from young and aged mice (Figures 3a and b). In tissues from each group, high levels of RANKL expression were specifically restricted to stromal cells in the SED. Similarly, no significant difference in the expression of *Tnfsf11* (which encodes RANKL), *Tnfrsf11a* (which encodes the RANKL receptor, RANK) or *Tnfrsf11b* (which encodes the RANKL decoy receptor osteoprotegerin, OPG) mRNA levels were detected in Peyer's patches from young or aged mice (Figures 3c-e, respectively). Thus, the effects of ageing on M cell status were not due to reduced expression of RANKL or RANK, or impaired RANKL-RANK stimulation due to elevated expression of OPG.

Cells within the FAE have a limited life-span of approximately 5 days and are constantly replaced by those which differentiate and migrate from stem cells within the dome-associated crypts adjacent to the GALT[16]. We therefore determined whether ageing affected cell proliferation. IHC analysis showed that whereas there was a dramatic reduction in the number of proliferating cells ($Ki\text{-}67^+$ cells) in the Peyer's patch follicles of aged mice, no difference was observed in the dome-associated crypts (Supplementary Figure 1). Similarly, aging was not associated with increased levels of apoptosis in the FAE. Apoptotic cells were rare in the FAE of young and aged mice. As anticipated, tingible body macrophages in the B cell follicles contained large numbers of $TUNEL^+$ (apoptotic) cells (Supplementary Figure 2)[17].

Ageing impairs the maturation of M cells

Annexin A5 (ANXA5) is also a specific marker for M cells in the FAE[18]. The systemic treatment of mice with RANKL induces the differentiation of RANK-expressing villous enterocytes into M cells[2]. Consistent with this role, analysis of microarray data from the intestines of RANKL-treated mice[4] shows that by 6 h, a significant increase in *Anxa5* mRNA expression was observed in the villous epithelium reaching peak levels by 48 h

Europe PMC Funders Author Manuscripts

Europe PMC Funders Author Manuscripts

(Figure 4a). However, *Gp2* expression was not induced until 48 h after exposure (Figure 4a). These data show that GP2 is restricted to more mature M cells, whereas ANXA5 is also expressed by immature/differentiating M cells[3, 4]. Ageing did not significantly influence the expression level of *Anxa5* mRNA (Figure 4b). As anticipated, many $GP2^+$ $ANXA5^+$ M cells were detected by IHC in the FAE of Peyer's patches of young mice (Figure 4c). However, consistent with the mRNA expression data (*Gp2*, Figure 1c; *Anxa5*, Figure 4b) our double IHC analysis showed that whereas the expression of GP2 was significantly reduced in the aged FAE (Figures 4c and d; $P < 0.0001$, Mann-Whitney U test), the expression of ANXA5 was unaffected (Figures 4c and e; $P = 0.340$, Student's t-test). These data show that ageing specifically affects the differentiation of immature $ANXA5^+$ cells into functionally mature $GP2^+$ M cells.

Expression of the Ets transcription factor Spi-B is reduced in the FAE of aged mice

The maturation of M cells has been shown to be mediated by their intrinsic expression of the Ets transcription factor Spi-B[4]. Cells in the FAE of Peyer's patches from Spi-B-deficient mice express equivalent levels of the immature M-cell marker ANXA5 to wild-type mice, but lack expression of mature M-cell markers such as GP2 and are defective in their ability to transcytose antigens[4]. Since these characteristics were similar to those observed in the aged FAE, we examined whether the reduced maturation of M cells in aged mice was due to effects on Spi-B expression. Our analysis showed that whereas large numbers of $Spi\text{-}B^+$ cells were detected throughout the FAE of young mice, they were significantly reduced in the FAE of aged mice (Figure 5; $P < 0.0001$, Student's t-test).

Ageing dramatically impairs the expression of CCL20 by the FAE

The FAE-specific expression of the chemokine CCL20 also plays an important role in M-cell differentiation. CCL20 mediates the chemoattraction of CCR6-expressing lymphocytes and leukocytes towards the FAE[19]. In the absence of CCL20-CCR6 stimulation M-cell maturation is impaired[20]. In young mice, as anticipated, dense CCL20-specific immunolabeling was detected exclusively in association with the FAE. However, CCL20 expression was significantly reduced in the FAE of aged mice (Figure 6a and b; $P < 0.0001$, Student's t-test). Whole mount *in situ* hybridisation analysis also demonstrated a substantial reduction in the expression of *Ccl20* mRNA in the FAE of aged mice (Figure 6c). CCR6-deficient mice display a comparable reduction in the density of mature $GP2^+$ M-cells in the FAE[20] to that observed in aged mice in the current study. Whether CCR6-deficiency affects the initial induction of M-cell development in the FAE and their expression of immature M-cell markers such as ANXA5 is not known. Our analysis revealed that the expression of ANXA5 in the FAE of $CCR6^{-/-}$ mice was unaffected when compared to wild-type mice (Supplementary Figure 3). These data show that as observed in aged mice, CCL20-CCR6-signaling blockade in $CCR6^{-/-}$ mice does not affect the initial induction of M cell differentiation (expression of ANXA5; Supplementary Figure 3), but specifically impedes their maturation (expression of GP2 and ability to transcyose Ag)[20]. Together, these data suggest that the effects of aging on the functional maturation of M cells were also due to impaired CCL20 expression by the FAE.

Pathogen-associated molecular patterns (PAMP) derived from intestinal bacteria, such as LPS and flagellins, can modulate cytokine and chemokine expression by intestinal epithelial cells via stimulation through Toll-like receptors (TLR). Since flagellin can induce CCL20 expression in the intestinal epithelium via stimulation through TLR5[21, 22], we determined whether the intestinal concentrations of proinflammatory bacterial TLR ligands were altered in aged mice. Sterile-filtered faecal (SFE) extracts were prepared as representative samples of the soluble PAMP in the gut lumen of mice from each age group. PAMP specific for TLR4 (LPS equivalents) and TLR5 (flagellin equivalents) in SFE were quantified using

Europe PMC Funders Author Manuscripts

Europe PMC Funders Author Manuscripts

HEK-293 cells transfected with the respective TLRs and calibrated with defined standard PAMP[23]. Our analysis showed that ageing did not significantly alter the intestinal concentrations of proinflammatory ligands of TLR4 and TLR5 (Supplementary Figures 4a and b). Similarly, no significant difference was observed in the ability of the PAMP within SFE form young and aged mice to induce CCL20 mRNA expression in *in vitro*-cultivated Caco-2 intestinal epithelial cells (Supplementary Figure 4c). These data suggest that the effects of ageing on CCL20 expression in the FAE were not due to alterations to the PAMP profile of the gut microbiota.

The density of CD11c$^+$ B cells in the FAE of aged mice is significantly reduced

A unique subset of CCR6-expressing "M-cell-inducing" CD11c$^+$ B cells has been shown to migrate towards FAE-derived CCL20 and play an important role in stimulating M cell-differentiation[20]. We therefore compared the distribution of T cells, B cells and CD11c$^+$ cells in the FAE of young and aged mice. Coincident with the effects of ageing on CCL20 expression, the density of T cells (CD3$^+$ cells; Figures 7a and b; $P < 0.014$, Student's t-test) and B cells (CD45R$^+$ cells; Figures 7c and d; $P < 0.025$, Student's t-test) was significantly reduced in the FAE of aged mice. Although no significant difference in the total density of CD11c$^+$ cells was observed (Figures 7e and f; $P = 0.656$, Student's t-test), our data implied that the density of CD11c$^+$ B cells was significantly reduced in the FAE of aged mice (CD11c$^+$ CD45R$^+$ cells; Figures 7g and h; $P < 0.020$, Student's t-test). The density of the CD11c$^+$ B cells in the aged FAE appeared to be more profoundly decreased than that of the conventional B cells (38% and 65% density observed in young mice, respectively), consistent with the higher expression level of CCR6 on CD11c$^+$ B cells[20]. The CD11c$^+$ CD45R$^+$ cells were not plasmacytoid DC as they lacked expression of the typical plasmacytoid DC markers PDCA-1 and Gr-1 (Figures 7i and j). Together, these data show that as a consequence of the impaired CCL20 expression in the Peyer's patches of aged mice fewer B cells are attracted towards the FAE (including those which appeared to express CD11c), potentially impeding their ability to stimulate M-cell-differentiation.

DISCUSSION

Here we show that the density of M cells in FAE of aged mice is dramatically reduced, significantly impeding the transcytosis of particulate antigen across the gut epithelium. Ageing specifically impaired the expression of Spi-B and down-stream functional maturation of M cells. Expression of the chemokine CCL20 was also reduced in the FAE of aged mice, impeding the attraction of B cells towards the FAE. The M-cell intrinsic expression of Spi-B[4] and CCL20-mediated attraction of CCR6-expressing CD11c$^+$ B cells towards the FAE[20] each play important roles in the induction of M-cell differentiation. Taken together, these data suggest that the effects of ageing on Spi-B and CCL20 expression in the FAE dramatically impede the functional maturation of M cells in Peyer's patches. Data in the current study reveal an important ageing-related deficiency in the mucosal immune system's ability to sample lumenal antigens.

The expression of high levels of RANKL by stromal cells directly beneath the FAE plays a critical role in controlling the differentiation of M cells from intestinal epithelial precursor cells[2]. In the absence of RANKL, M-cell differentiation is blocked. Since RANKL is a critical factor that provides the initial stimulus to trigger the differentiation of M cells from RANK-expressing enterocytes, we compared the expression levels of RANKL and RANK in young and aged Peyer's patches. However, the expression of RANKL and RANK was not adversely affected in aged mice. This indicates that factors down-stream of RANKL-RANK signalling are responsible for the impaired M cell development in aged mice. OPG is a secreted decoy receptor of RANKL and its enhanced expression can suppress RANKL-

Europe PMC Funders Author Manuscripts

Europe PMC Funders Author Manuscripts

stimulation[24]. However, our data show that the relative expression levels of OPG and RANKL were not influenced in the Peyer's patches of aged mice.

ANXA5 and GP2 are both specifically expressed by M cells[3, 13, 18]. Analysis of the effects of RANKL stimulation on gene expression in the villous epithelium showed that whereas *Anxa5* was rapidly induced within hours of exposure, *Gp2* was induced at a much later time after treatment[4]. These data support the view that GP2 is restricted to terminally-differentiated M cells and also indicate that ANXA5 is expressed by immature (and mature) M cells[3, 4, 18]. These data also suggest that the expression of *Anxa5* and *Gp2* are regulated by different transcriptional mechanisms: *Anxa5* expression in the intestinal epithelium is rapidly induced by RANKL-stimulation whereas *Gp2* is not directly induced by RANKL-stimulation. The expression of ANXA5 in the FAE of aged mice was unaffected, indicating that the RANKL-RANK signalling events leading to ANXA5 expression were not influenced by ageing. However, GP2 expression was significantly impaired. These data show that ageing does not affect the induction of M cell differentiation, but specifically impedes their maturation. These data also show that RANKL-stimulation is critical for the induction of M cell differentiation, whereas RANKL-stimulation alone is insufficient to maintain their functional maturation.

M-cell intrinsic expression of the Ets transcription factor Spi-B is essential for their functional maturation and expression of mature M-cell markers such as GP2[4]. However, the expression of early M-cell markers including ANXA5 is independent of Spi-B. In the current study similar effects on the functional maturation of M cells were observed in the FAE of aged mice to those observed in Spi-B-deficient mice. Expression of ANXA5 was comparable in young and aged mice, but the expression of Spi-B and the mature M-cell marker GP2 was significantly reduced. Furthermore, as observed in the Peyer's patches of Spi-B-deficient mice, the residual ANXA5$^+$ cells in the FAE of aged mice were defective in their ability to transcytose particulate antigen from the gut lumen. These data suggest ageing adversely affects the induction and/or maintenance of Spi-B expression, impairing the functional maturation of M cells.

Lymphoepithelial interactions also promote M-cell differentiation[20]. A unique subset of M-cell inducing CCR6-expressing CD11c$^+$ B cells has been shown to migrate towards FAE-derived CCL20 and play an important role in stimulating M cell differentiation[20]. Mice deficient in CCR6, the sole receptor for CCL20, have a reduced frequency of mature GP2$^+$ M cells in the FAE[20]. In the current study the reduced expression of Spi-B and impaired functional maturation of M cells coincided with a similar reduction in CCL20 expression by the FAE. Indeed, the CCR6-deficient mice show a comparable reduction in the density of mature M cells in the FAE[20] to that observed in aged mice (current study). We also show that as observed in aged mice, CCR6-deficiency did not affect the expression of immature M cell markers such as ANXA5, but specifically impeded their maturation. Together, these data suggest that the effects of aging on the functional maturation of M cells were also a consequence of the reduced CCL20 expression, impeding the migration of B cells (including those which appeared to express CD11c) towards the FAE [20].

The underlying mechanism responsible for the reduced expression of Spi-B and CCL20 in the Peyer's patches of aged mice which ultimately impede the functional maturation of M cells in the FAE is uncertain. Our data show these effects were not due to reduced cell proliferation in the dome-associated crypts, increased apoptosis in the FAE, impaired RANKL-RANK stimulation due to elevated expression of the RANKL decoy receptor OPG, or alterations to the concentrations of proinflammatory ligands of TLR4 and TLR5 in the intestine.

Europe PMC Funders Author Manuscripts

Europe PMC Funders Author Manuscripts

Data in the current study provide an important advance in our understanding of the effects of ageing on the mucosal immune system. The effective uptake of antigens by M cells is an important initial step in the induction of an efficient immune response to some microorganisms or after oral vaccination. Our data show that due to the reduced density of mature M cells in the FAE, the uptake of particulate antigen from the gut lumen is significantly compromised in aged individuals. Antigen-specific mucosal immune responses are markedly diminished in Spi-B-deficient[4] and CCR6-deficient mice[19] which display a dramatic reduction in the density of mature M cells in the FAE[4, 20]. Furthermore, CCR6-deficient mice display a similar reduction in M cell density to that observed in aged mice in the current study. Similarly, in the absence of GP2-expression by M cells, antigen-specific IgA responses against type-1 piliated bacteria are also attenuated[13]. This suggests that the effects of aging on the functional maturation of M cells and their expression of GP2 may significantly contribute to the impaired antigen-specific mucosal immune responses observed in aged mice[6]. The targeted delivery of vaccine antigens to M cells is an effective means of inducing antigen-specific mucosal immune responses to certain antigens[10, 11]. Data in the current study suggest that such strategies may be less effective when used to immunize the elderly. However, the effects of ageing on M-cell status may also reduce susceptibility to some pathogens that specifically exploit M cells to infect the host[25-29]. For example, M cells are important sites of prion uptake from the gut lumen and disease susceptibility after oral exposure is blocked in their absence[29]. Susceptibility to oral prion infection is dramatically reduced in aged mice[30]. Thus it is plausible that the effects of ageing on M-cell maturation may reduce susceptibility to orally-acquired prion infection by impeding their initial uptake into Peyer's patches. The enteroinvasive bacterium *Salmonella* Typhimurium is also considered to exploit M cells to establish infection after oral exposure[26] and its translocation into Peyer's patches is impeded in the absence of M cells[4] or their expression of GP2[13]. The significantly reduced early uptake of *S.* Typhimurium into the Peyer's patches of aged mice[31] may likewise be a consequence of the effects of ageing on M-cell status. A thorough analysis of the molecular mechanisms that underpin the dramatic decline in the functional maturation of M cells in aged mice will aid our understanding of the factors that influence susceptibility to mucosally-acquired pathogens and identify novel approaches to stimulate M cell differentiation and improve mucosal immunity in the elderly.

METHODS

Mice

C57BL/6J mice were aged to at least 18 months old prior to analysis. Six- to 8-week old C57BL/6J mice were used as young adults. All mice from each group received identical diets and were housed and maintained under identical SPF conditions. Throughout this study tissues from at least 3 independent cohorts of young and aged mice were analysed. CCR6-EGFP knock-in mice[32] were backcrossed onto C57BL/6J mice for at least eight generations prior to analysis. All studies using experimental mice and regulatory licences were approved by the following authorities: UK, the University of Edinburgh's Ethical Review Committee and performed under the authority of a UK Home Office Project Licence within the regulations of the UK Home Office 'Animals (scientific procedures) Act 1986'; Japan, by the Animal Research Committee of the RIKEN Yokohama Research Institute.

IHC analyses

For whole-mount staining, Peyer's patches were dissected and fixed with BD Cytofix/Cytoperm (BD Biosciences, Oxford, UK). Tissues were subsequently immunostained with rat anti-mouse GP2 mAb (MBL International, Woburn, MA). Following addition of primary Ab, tissues were stained with Alexa Fluor 488-conjugated anti-rat IgG Ab (Invitrogen,

Europe PMC Funders Author Manuscripts

Europe PMC Funders Author Manuscripts

Paisley, UK), rhodamine-conjugated *Ulex europaeus* agglutinin I (UEA-1; Vector Laboratories Inc., Burlingame, CA) and Alexa Fluor 647-conjugated phalloidin (Invitrogen).

For analysis of tissue sections, Peyer's patches were removed and snap-frozen at the temperature of liquid nitrogen. Serial frozen sections (5 μm in thickness) were immunostained with the following antibodies: rat anti-mouse GP2 mAb to detect M cells; rat anti-mouse CD254 to detect RANKL (clone IK22/5; eBioscience, Hatfield, UK); rabbit anti-Ki67 polyclonal Ab (Abcam, Cambridge, UK); rabbit anti-annexin V polyclonal Ab (Abcam); biotinylated hamster anti-mouse (CD3e mAb (clone 500-A2; Caltag-Medsystems, Buckingham, UK); Alexa-Fluor 488-conjugated rat anti-mouse CD45R (B220) mAb (clone RA3-6B2; Invitrogen); rat anti-mouse PDCA-1 mAb (clone JF05-1C2.4.1; Miltenyi Biotec, Surrey, UK); rat anti-mouse Ly-6G (Gr-1) mAb (clone RB6-8C5; eBioscience); biotinylated hamster anti-mouse CD11c (clone HL3; BD Biosciences). For the detection of CCL20, tissues were first fixed in 4% paraformaldehyde prior to sectioning and immunostaining with goat anti-mouse CCL20 polyclonal Ab (R&D Systems, Abingdon, UK). For the detection of Spi-B in paraformaldehyde-fixed sections, antigen retrieval was performed with citrate buffer (pH 7.0, 121°C, 5 min.) prior to immunostaining with sheep anti-mouse Spi-B polyclonal Ab (R&D Systems). Appropriate species and immunoglobulin isotype control Ab were used as controls (Supplementary Figure 5). Unless indicated otherwise, following the addition of primary antibody, species-specific secondary antibodies coupled to Alexa Fluor 488 (green) and Alexa Fluor 555 (red) dyes were used (Invitrogen). Sections were mounted in fluorescent mounting medium (Dako, Ely, UK) and examined using a Zeiss LSM5 confocal microscope (Zeiss, Welwyn Garden City, UK).

In vivo assessment of M cell-mediated transcytosis

The *in vivo* uptake of 200 nm diameter fluoresbrite YG carboxylate microspheres (Polysciences, Eppelheim, Germany) from the gut lumen was assessed using a gut-loop model as described[2]. Briefly, to prepare isolated small intestinal loops, mice were anesthetized and segments of small intestine (~2 cm in length) containing a single Peyer's patch were tied off with nylon filament. The loops were then injected with 200 μl of a suspension of 200 nm fluorescent nanoparticles diluted in PBS (1×10^{11} beads/ml). The isolated gut loops were then placed back in the peritoneal cavity. Approximately 1 h later the injected gut loops were excised, washed in 0.5% Tween 20-PBS, fixed in 4% paraformaldehyde in PBS, and embedded in OCT. Frozen sections (5 μm in thickness) were counter-stained with Alexa Fluor 647-conjugated phalloidin to detect f-actin and examined using a fluorescence microscope. Data were collected from 10 sections from each Peyer's patch.

Image analysis

For morphometric analysis, digital microscopy images were analyzed using ImageJ software (http://rsb.info.nih.gov/ij/) as described[33]. All images were coded and assessed blindly. Background intensity thresholds were first applied using an ImageJ macro which measures pixel intensity across all immunostained and non-stained areas of the images. The obtained pixel intensity threshold value was then applied in all subsequent analyses. Next, the number of pixels of each colour (black, red, green, yellow) were automatically counted and presented as a proportion of the total number of pixels in each area under analysis. In each instance, tissues from at least 4 mice from each group were analyzed. In order to analyse the expression of several paramaters from each mouse, multiple sections from at least 3 Peyer's patches were analyzed and the numbers of positively immunostained pixels in images of specific Peyer's patch regions were collected.

Europe PMC Funders Author Manuscripts

Europe PMC Funders Author Manuscripts

Quantitative real-time PCR analysis of mRNA expression

Total RNA was isolated from Peyer's patches using the RNA-Bee (AMS Biotechnology, Oxfordshire, UK) followed by treatment with DNase I (Ambion, Warrington, UK). First strand cDNA synthesis was performed using 1 μg of total RNA and the First Strand cDNA Synthesis kit (GE Healthcare, Bucks, UK) as described by the manufacturer. PCR amplification reactions were performed using the Platinum-SYBR Green qPCR SuperMix-UDG kit (Invitrogen) and the Stratagene Mx3000P real-time qPCR system (Stratagene, CA, USA). All qPCR primers used were designed using Primer3 software[34] and their details are provided in Supplementary Table 1. The cycle threshold values were determined using MxPro software (Stratagene) and normalized to the value of *Actb*.

Whole-mount RNA *in situ* hybridisation

A 721 bp DNA fragment of the mouse *Ccl20* gene was amplified from cDNA derived from mouse Peyer's patches by PCR using primers 5′-ACCCAGCACTGAGTACATCAAC-3′ (forward) and 5′-GAAAATCATATCAATTTAAGAAGCAA-3′ (reverse) and subcloned into pGEM-T Easy vector (Promega, Southampton, UK). Digoxigenin (DIG)-labelled sense and anti-sense RNA probes were synthesized using the DIG-RNA labelling kit with SP6 and T7 RNA polymerases (Roche Diagnostics, West Sussex, UK). Whole-mount *in situ* hybridisation on Peyer's patches was performed as described[35].

Measurement of relative biological activities of PAMP in SFE

SFE from faecal pellets of individual mice were prepared as previously described[23]. PAMP concentrations in SFE from young and aged mice were quantified by measuring their capacity to induce NK-κB signalling in HEK-293 cells transfected with TLR4/MD2 or TLR5 as described[23]. Briefly, TLR-deficient HEK-293 cells were transfected 30 ng of human TLR4 (co-expressing MD2) or TLR5, 30 ng of CD14, 20 ng of renilla luciferase-reporter construct and 10 ng of firefly luciferase-reporter construct driven by the NF-κB-dependent E-selectin promoter. Cell were cultivated in DMEM/10% FCS (Sigma) and 3 days later cells were stimulated in duplicate with SFE, defined TLR-ligands (TLR4, *Eschericia coli* R1 [NCTC-13114]-derived LPS repurified to remove TLR2-stimulating lipopolypeptide contaminants; TLR5, flagellin of *Salmonella* Typhimurium) or whole heat-killed bacteria (HKB, derived from faecal samples) for 18 h. NF-κB-dependent reporter expression was then measured using Promega Dual-Glo reagent and normalised to co-transfected renilla expression. Fold induction was calculated relative to the cells cultivated in medium alone and a standard curve prepared by plotting the fold NF-κB-induction vs. concentration of each PAMP standard. To determine the relative PAMP abundance in SFE, samples were diluted until the induction of reporter occurred within the linear range of the standard curve. PAMP abundance in SFE is presented as ng PAMP/mg protein.

In parallel assays, human Caco-2 intestinal epithelial cells were stimulated in triplicate *in vitro* with SFE, HBK or medium alone (control). 2 h after treatment, cells were harvested and *CCL20* mRNA expression levels compared by quantitative real-time PCR analysis using the primers listed in Supplementary Table 1. Data were normalized to the expression level of *ACTB* and are presented relative to the expression level in unstimulated (medium alone control) cells.

Statistical analyses

Data are presented as mean ± SD. Unless indicated otherwise, differences between groups were analysed by a Student's t-test. In instances where there was evidence of non-normality, data were analysed by a Mann-Whitney U test. Values of $P < 0.05$ were accepted as significant.

Europe PMC Funders Author Manuscripts

Europe PMC Funders Author Manuscripts

Supplementary Material

Refer to Web version on PubMed Central for supplementary material.

Acknowledgments

We thank Simon Cumming, Megan Davey, Bob Fleming, Fraser Laing, and the Pathology Services Group (University of Edinburgh, UK) for excellent technical support, Helen Brown (University of Edinburgh, UK) for statistical advice and Gaku Nakato (RCAI-RIKEN, Yokohama, Japan) for excellent technical advice and helpful discussion. This work was supported by project (BB/J014672/1) and Institute Strategic Programme Grant (BB/J0004332/1) funding from the Biotechnology and Biological Sciences Research Council. A.K. is supported by a Japan Society for the Promotion of Science Fellowship for Research Abroad and natural sciences grant funding from the Mitsubishi Foundation.

REFERENCES

1. Krahenbuhl JP, Neutra MR. Epithelial M cells: differentiation and function. Annu. Rev. Cell Dev. Biol. 2000; 16:301–332. [PubMed: 11031239]
2. Knoop KA, et al. RANKL is necessary and sufficient to initiate development of antigen-sampling M cells in the intestinal epithelium. J. Immunol. 2009; 183:5738–5747. [PubMed: 19828638]
3. Nakato G, et al. New approach for M-cell-specific molecules by screening comprehensive transcriptome analysis. DNA Res. 2009; 16:227–235. [PubMed: 19675110]
4. Kanaya T, et al. The Ets transcription factor Spi-B is essential for the differentiation of intestinal microfold cells. Nat. Immunol. 2012; 13:729–736. [PubMed: 22706340]
5. Schmucker D, Owen R, Outenreath R, Thoreux K. Basis for the age-related decline in intestinal mucosal immunity. Clinical and Developmental Immunology. 2003; 10:167–172. [PubMed: 14768948]
6. Koga T, et al. Evidence for early aging in the mucosal immune system. J. Immunol. 2000; 165:5352–5359. [PubMed: 11046071]
7. Kato H, et al. Lack of oral tolerance in ageing is due to sequential loss of Peyer's patch cell interactions. Int. Immunol. 2003; 15:145–158. [PubMed: 12578844]
8. Fujihashi K, McGhee JR. Mucosal immunity and tolerance in the elderly. Mechanisms of Ageing and Development. 2004; 125:889–898. [PubMed: 15563935]
9. Dunn-Walters DK, Banerjee M, Mehr R. Effects of age in antibody affinity maturation. Biochemical Society Transactions. 2003; 31:447–448. [PubMed: 12653658]
10. Nochi T, et al. A novel M cell-specific carbohydrate-targeted mucosal vaccine effectively induces antigen-specific immune responses. J. Exp. Med. 2007; 204:2789–2796. [PubMed: 17984304]
11. Misumi S, et al. Targeted delivery of immunogen to primate m cells with tetragalloyl lysine dendrimer. J. Immunol. 2009; 182:6061–6070. [PubMed: 19414757]
12. Terahara K, et al. Comprehensive gene expression profiling of Peyer's patch M cells, villous M-like cells, and intestinal epithelial cells. J. Immunol. 2008; 180:7840–7846. [PubMed: 18523247]
13. Hase K, et al. Uptake through glycoprotein 2 of $FimH^{+}$ bacteria by M cells initiates mucosal immune responses. Nature. 2009; 462:226–231. [PubMed: 19907495]
14. Kawanishi H, Kielly J. Immune-related alterations in aged gut-associated lymphoid tissues in mice. Digestive Dis. Sci. 1989; 34:175–184.
15. Pappo J, Ermak TH. Uptake and translocation of fluorescent latex particles by Rabbit Peyer's patch follicle-associated epithelium: a quantitative model for M cell uptake. Clin. Exp. Immunol. 1989; 76:114–148.
16. Gebert A, Fassbender S, Werner K, Weissferdt A. The development of M cells in Peyer's patches is restricted to specialized dome-associated crypts. Am. J. Pathol. 1999; 154:1573–1582. [PubMed: 10329609]
17. Kranich J, et al. Follicular dendritic cells control engulfment of apoptotic bodies by secreting Mfge8. J. Exp. Med. 2008; 205:1293–1302. [PubMed: 18490487]
18. Verbrugghe P, et al. Murine M cells express annexin V specifically. J. Pathol. 2006; 209:240–249. [PubMed: 16552796]

Europe PMC Funders Author Manuscripts

19. Cook DN, et al. CCR6 mediates dendritic cell localization, lymphocyte homeostasis, and immune responses in mucosal tissue. Immunity. 2000; 12:495–503. [PubMed: 10843382]
20. Ebisawa M, et al. CCR6^{hi}CD11c^{int} B cells promote M-cell differentiation in Peyer's patch. Int. Immunol. 2011; 23:261–269. [PubMed: 21422150]
21. Bambou J-C, et al. *In vitro* and *ex vivo* activation of the TLR5 signaling pathway in intestinal epithelial cells by a commensal *Eschericia coli* strain. J. Biol. Chem. 2004; 279:42984–42992. [PubMed: 15302888]
22. Sirard J-C, Didierlaurent A, Cayet D, Sierro F, Rumbo M. Toll-like receptor 5- and lymphotoxin b receptor-dependent epithelial cell Ccl20 expression involves the same NF-κB binding site but distinct NF-κB pathways and dynamics. Biochem. Biophys. Acta. 2009; 1789:386–294. [PubMed: 19303953]
23. Erridge CE, Duncan SH, Bereswill S, Heimesaat MM. The induction of colitis and ileitis in mice is associated with marked increases in intestinal concentrations of stimulants of TLRs 2, 4, and 5. PLoS One. 2010; 5:e9125. [PubMed: 20161736]
24. Trouvin A-P, Goeb V. Receptor activator of nuclear factor-κB ligand and osteoprotegerin: maintaining the balance to prevent bone loss. Clin. Interventions Aging. 2010; 5:345–354.
25. Amerongen HM, et al. Transepithelial transport of HIV-1 by intestinal M cells: a mechanism for transmission of AIDS. J Acquir Immune Defic Syndr. 1991; 4:760–765. [PubMed: 1856788]
26. Jones B, D, Ghori N, Falkow S. Salmonella typhimurium initiates murine infection by penetrating and destroying the specialized epithelial M cells of the Peyer's patches. J. Exp. Med. 1994; 180:15–23. [PubMed: 8006579]
27. Neutra MR, Frey A, Kraehenbuhl J-P. Epithelial M Cells: Gateways for Mucosal Infection and Immunization. Cell. 1996; 86:345–348. [PubMed: 8756716]
28. Sansonetti PJ, Phalipon A. M cells as ports of entry for enteroinvasive pathogens: mechanisms of interaction, consequences for the disease process. Seminars Immunol. 1999; 11:193–203.
29. Donaldson DS, et al. M cell depletion blocks oral prion disease pathogenesis. Mucosal Immunol. 2012; 5:216–225. [PubMed: 22294048]
30. Brown KL, Wathne GJ, Sales J, Bruce ME, Mabbott NA. The effects of host age on follicular dendritic cell status dramatically impair scrapie agent neuroinvasion in aged mice. J. Immunol. 2009; 183:5199–5207. [PubMed: 19786551]
31. Ren Z, et al. Effect of age on susceptibility to *Salmonella* Typhimurium infection in C57BL/6 mice. J. Med. Microbiol. 58:1559–1567. (20009). [PubMed: 19729455]
32. Kucarzik T, Hudson JT 3rd. Waikel RL, Martin WD, Williams IR. CCR6 expression distinguishes mouse myeloid and lymphoid dendritic cell subsets: demonstration using a CCR6 knock-in mouse. Eur. J. Immunol. 2002; 32:104–112. [PubMed: 11754009]
33. Inman CF, et al. Validation of computer-assisted, pixel-based analysis of multiple-colour immunofluorescence histology. Journal of Immunological Methods. 2005; 302:156–167. [PubMed: 15992812]
34. Untergasser A, et al. Primer3Plus, an enhanced web interface to Primer3. Nucleic Acids Res. 2007; 35:W71–W74. [PubMed: 17485472]
35. Nieto MA, Patel K, Wilkinson DG. Chapter 11 *In situ* hybridization analysis of chick embryos in whole mount and tissue sections. Met. Cell. Biol. 1996; 51:219–235.

Europe PMC Funders Author Manuscripts

Europe PMC Funders Author Manuscripts

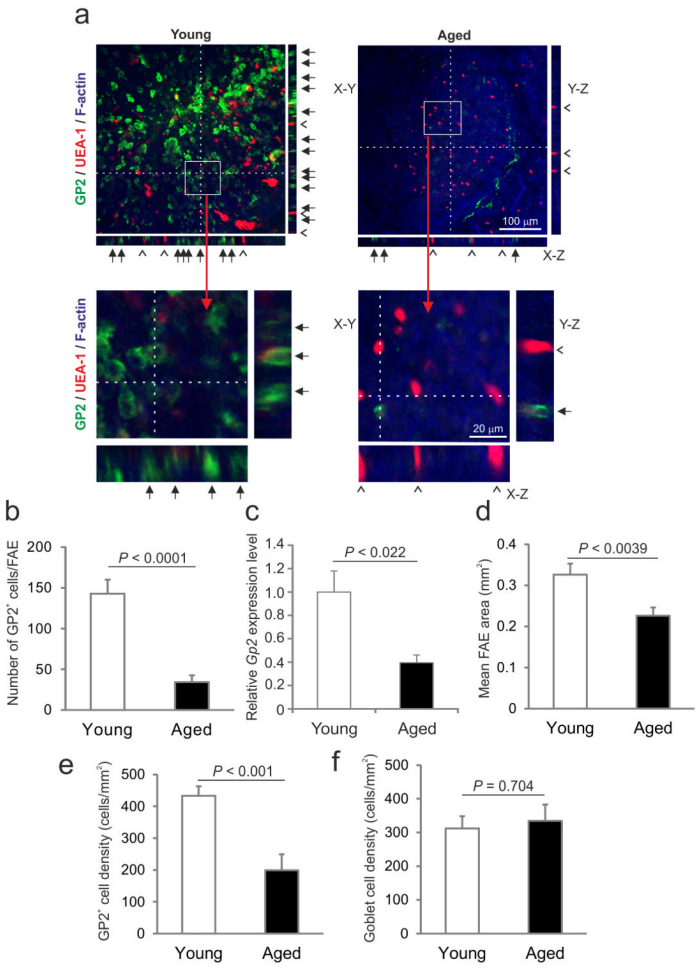

Figure 1.

M-cell density is significantly reduced in the FAE of Peyer's patches from aged mice. (a) Tissues were immunostained to detect GP2 (green), UEA-1 (red) and f-actin (blue). The positions of the X-Z and Y-Z projections of the FAE are indicated by the broken line in the main X-Y images. Closed arrows indicate $GP2^+$ M cells with characteristic basolateral pockets. Open arrow-heads indicate $GP2^-$ $UEA\text{-}1^+$ goblet cells. The boxed areas in each of the main X-Y images are shown below at higher magnification. (b) Morphometric analysis indicated that the number of $GP2^+$ M cells in the FAE of aged mice was significantly reduced ($P < 0.0001$, Mann-Whitney U test). (c) Real-time RT-qPCR analysis revealed a significant reduction in *Gp2* transcript levels in tissues from aged mice ($P < 0.022$, Student's t-test). Gene expression data are normalised so that the mean level in young mice was 1.0. (d) Morphometric analysis suggested that the size of the FAE in Peyer's patches of aged mice was smaller than those in young mice ($P < 0.039$, Student's t-test). (e) The density of M cells in the FAE of aged mice was significantly reduced ($P < 0.001$, Mann-Whitney U test). (f) Ageing did not influence the density of $GP2^-$ $UEA\text{-}1^+$ goblet cells in the FAE ($P = 0.707$, Student's t-test). Data are derived from 3-5 Peyer's patches from 4 mice from each group.

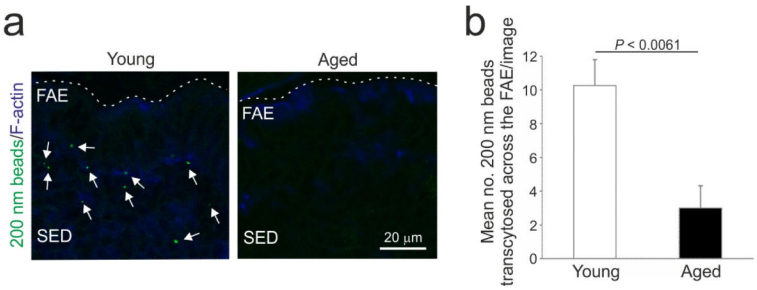

Figure 2.

The uptake of particulate antigen into the Peyer's patches of aged mice is significantly impaired. (a) In Peyer's patches from young mice many fluorescent beads (arrows, green) had been transcytosed across the FAE. Substantially fewer, if any, beads appeared to have passed through the FAE of aged mice. Sections were counterstained to detect f-actin (blue). Broken line indicates the lumenal surface of the FAE. (b) The number of beads transcytosed across the FAE of aged mice was significantly less than that observed in Peyer's patches from young mice ($P < 0.0061$, Student's t-test). Data were collected from 10 sections from each Peyer's patch. Data are derived from 3-5 Peyer's patches from 4 mice from each group.

Europe PMC Funders Author Manuscripts
Europe PMC Funders Author Manuscripts

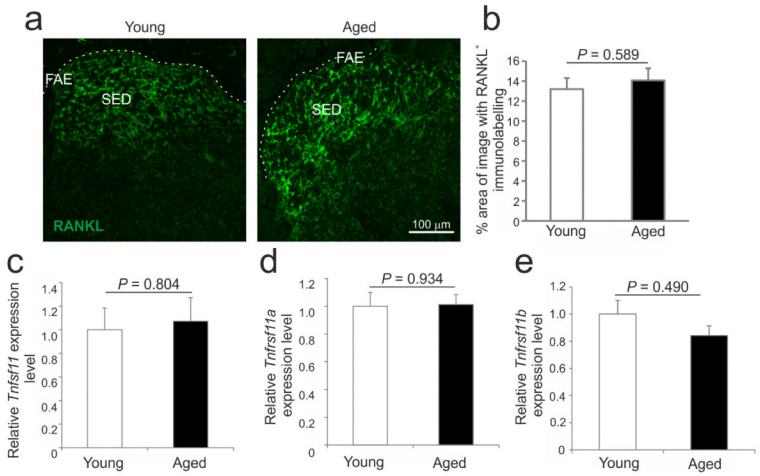

Figure 3.

Ageing does not influence the expression of RANKL, RANK and OPG in Peyer's patches. (a) IHC analysis suggested there was no observable difference in the expression or distribution of RANKL on SED stromal cells in Peyer's patches from young and aged mice. Broken line indicates the lumenal surface of the FAE. (b) Morphometric analysis confirmed that the magnitude of RANKL-specific immunostaining observed in the SED of Peyer's patches from young and aged mice was similar. Real-time RT-qPCR analysis suggested there was no significant difference in the expression of (c) *Tnfsf11* (RANKL), (d) *Tnfrsf11a* (RANK) or (e) *Tnfrsf11b* (OPG) mRNA levels between Peyer's patches from young or aged mice. Gene expression data are normalised so that the mean level in young mice was 1.0. Data are derived from 3-5 Peyer's patches from at least 4 mice/group.

Europe PMC Funders Author Manuscripts
Europe PMC Funders Author Manuscripts

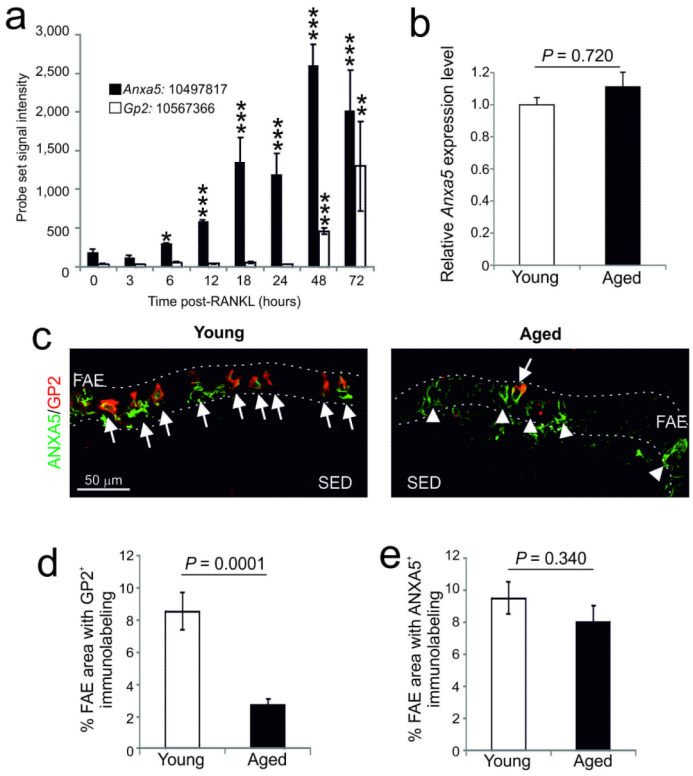

Figure 4.

Ageing does not affect the expression of ANXA5 in the FAE. (a) Effect of systemic rec-RANKL treatment on the expression of *Anxa5* (closed bars) and *Gp2* (open bars) in the villous epithelium. Each bar represents mean probe set signal intensity. The notation *XXXX*:12345678 represents *gene symbol*:Affymetrix probe set ID. *, $P < 0.05$; **, $P < 0.002$; $P < 0.0001$ (Student's t-test). (b) Real-time RT-qPCR analysis suggested there was no significant difference in the expression levels of *Anxa5* in young or aged mice. (c) IHC analysis of the expression of GP2 (red) and ANXA5 (green) by M cells in the FAE of young and aged mice. Arrows, $GP2^{+}ANXA5^{+}$ M cells; arrow-heads, $GP2^{-}ANXA5^{+}$ immature M cells. Broken lines indicate the boundary of the FAE. (d) Morphometric analysis confirmed that the magnitude of the GP2-specific immunostaining observed in the FAE of Peyer's patches from aged mice was significantly reduced when compared to young mice ($P < 0.0001$, Mann-Whitney U test). (e) However, ageing did not influence the magnitude of the ANXA5-specific immunostaining observed in the FAE ($P = 0.340$, Student's t-test). Data are derived from 3-5 Peyer's patches from at least 4 mice from each group.

Europe PMC Funders Author Manuscripts
Europe PMC Funders Author Manuscripts

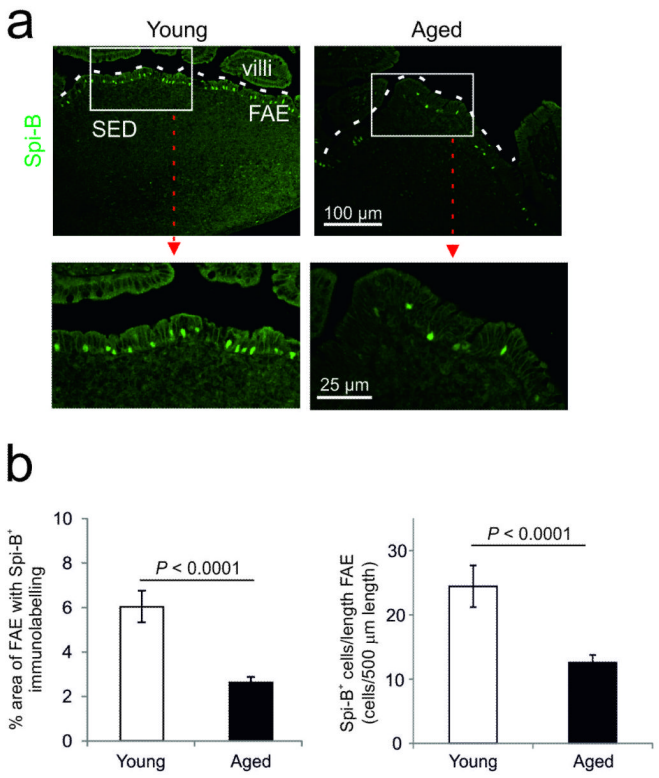

Figure 5.

Effects of ageing on Spi-B expression in the FAE of Peyer's patches. (a) IHC analysis suggested that Spi-B (green) was reduced in the FAE of aged mice. Boxed area in upper panels is shown at higher magnification in lower panels. Broken line indicates the lumenal surface of the FAE. (b) Morphometric analysis showed that the magnitude of the Spi-B-specific immunostaining and number of Spi-B$^+$ cells were significantly reduced in the FAE of aged mice ($P < 0.0001$, Student's t-test). Data are derived from 4-6 Peyer's patches from 8 mice from each group.

Europe PMC Funders Author Manuscripts
Europe PMC Funders Author Manuscripts

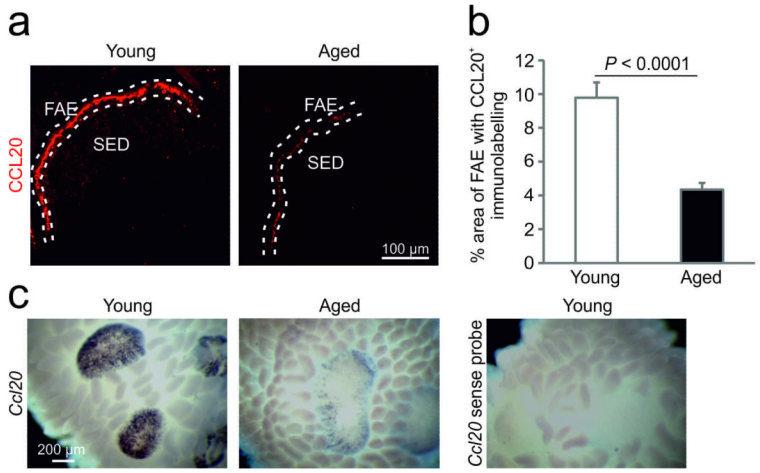

Figure 6.

Effects of ageing on CCL20 expression in the FAE of Peyer's patches. (a) IHC analysis suggested that CCL20 (red) was reduced in the FAE of aged mice. Broken line indicates the lumenal surface of the FAE. (b) Morphometric analysis showed that the magnitude of CCL20-specific immunostaining observed in aged mice was significantly reduced ($P < 0.0001$, Student's t-test). Data are representative of 3-5 Peyer's patches from 8 mice from each group. (c) Whole mount *in situ* hybridisation analysis demonstrated a dramatic reduction in *Ccl20* mRNA expression in the Peyer's patches of aged mice when compared to young mice. Data are derived from 21 Peyer's patches from each group.

Europe PMC Funders Author Manuscripts
Europe PMC Funders Author Manuscripts

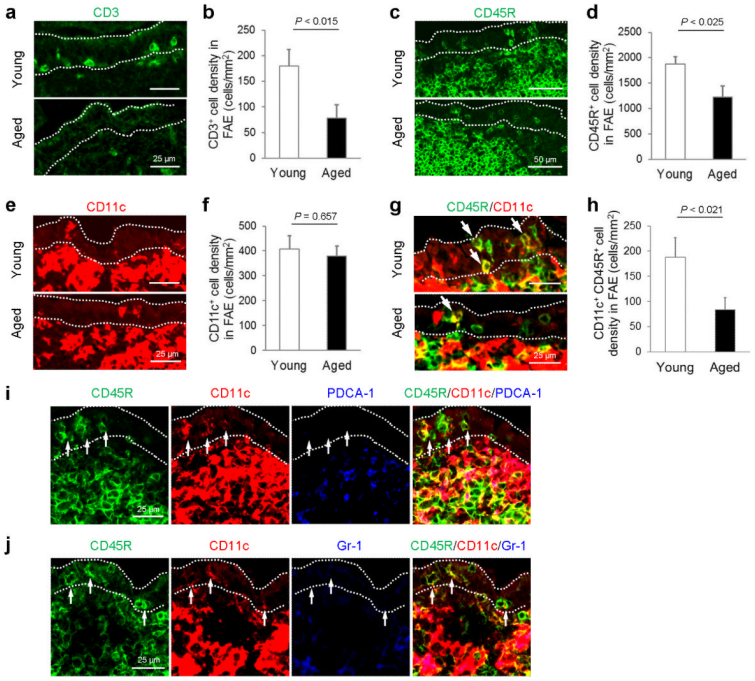

Figure 7.

The density of $CD11c^+$ B cells in the FAE of aged mice is significantly reduced. (a, c, e & g) IHC comparison of the distribution of T cells (panel a; $CD3^+$ cells; green), B cells (panel c; $CD45R^+$ cells, green), $CD11c^+$ cells (panel e; red) and $CD11c^+$ B cells (panel g, i and j) in the FAE of young and aged mice. Arrows in panel g indicate $CD11c^+$ B cells. (b, d, f & g) Morphometric analysis of the density of T cells (panel b; $CD3^+$ cells), B cells (panel d; $CD45R^+$ cells), $CD11c^+$ cells (panel f) and $CD11c^+$ B cells (panel h) in the FAE of young and aged mice. (I & j) IHC analysis confirmed that the $CD11c^+$ $CD45R^+$ cells were not plasmacytoid DC as they lacked expression of the typical plasmacytoid DC markers PDCA-1 (blue, panel i) and Gr-1 (blue, panel j). Data are derived from 3-5 Peyer's patches from 4 mice from each group.

Europe PMC Funders Author Manuscripts
Europe PMC Funders Author Manuscripts